Response of Coastal Phytoplankton to High Inflows of Terrestrial Matter

Paczkowska, Joanna

2020-02-28

Paczkowska , J , Brugel , S , Rowe , O , Lefebure , R , Brutemark , A & Andersson , A 2020 , ' Response of Coastal Phytoplankton to High Inflows of Terrestrial Matter ' , Frontiers in Marine Science , vol. 7 , 80 . https://doi.org/10.3389/fmars.2020.00080

http://hdl.handle.net/10138/317375
https://doi.org/10.3389/fmars.2020.00080

frontiers in Marine Science

ORIGINAL RESEARCH
published: 28 February 2020
doi: 10.3389/fmars.2020.00080

Response of Coastal Phytoplankton to High Inflows of Terrestrial Matter

Joanna Paczkowska[1,2†], Sonia Brugel[1,2], Owen Rowe[1,2,3†], Robert Lefébure[1,2†], Andreas Brutemark[4,5] and Agneta Andersson[1,2]*

[1] Department of Ecology and Environmental Science, Umeå University, Umeå, Sweden, [2] Umeå Marine Sciences Centre, Hörnefors, Sweden, [3] Department of Food and Environmental Sciences, Division of Microbiology and Biotechnology, University of Helsinki, Helsinki, Finland, [4] Novia University of Applied Sciences, Ekenäs, Finland, [5] Tvärminne Zoological Station, University of Helsinki, Hangö, Finland

Climate change scenarios project that precipitation will increase in northern Europe, causing amplified inflows of terrestrial matter (tM) and inorganic nutrients to coastal areas. How this will affect the plankton community is poorly understood. A mesocosm experiment was carried out to investigate the influence of two levels of tM inputs on the composition, size-structure and productivity of a natural coastal phytoplankton community from the northern Baltic Sea. The tM addition caused browning of the water and decreased underwater light levels, while the concentrations of dissolved organic carbon (DOC) and inorganic nutrients increased. Microphytoplankton were promoted by tM addition, while in the controls picophytoplankton dominated the phytoplankton community. Inorganic nutrient availability was instrumental in defining the phytoplankton community composition and size-structure. As a response to tM addition, the phytoplankton increased their chlorophyll *a* content. This physiological adaptation helped to maintain high primary production rates at the low tM enrichment, but at the high tM load the primary production decreased as did the biomass of mesozooplankton. The ciliate biomass was high when the mesozooplankton biomass was low, indicating that a trophic cascade occurred in the system. Structural equation modeling showed that tM borne DOC promoted ciliates, while primary and bacterial production were disfavored. Thus, DOC originating from soils had an indirect negative effect on the mesozooplankton by reducing their food availability. Although, a positive correlation between heterotrophic bacteria and phytoplankton suggested coupling between phytoplankton produced carbon and heterotrophs growth. The results from our study indicate that river-borne DOC and inorganic nutrients have a large impact on the phytoplankton community, driving the system to the dominance of large diatoms. However, since river-borne humic substances cause browning of the water, phytoplankton increase their light harvesting pigments. At moderate inflow this helps to support the primary production, but at high inflows of terrestrial material the primary production will decrease. As high river inflows have been projected to be a consequence of climate change, we foresee that primary production will decrease in coastal areas in the future, and the impacts of such changes on the food web could be significant.

Keywords: coastal phytoplankton, terrestrial organic matter, climate change, primary production, chlorophyll *a*

OPEN ACCESS

Edited by:
Hans Paerl,
University of North Carolina at Chapel Hill, United States

Reviewed by:
Patricia M. Glibert,
University of Maryland Center for Environmental Science (UMCES), United States
Sibel Bargu,
Louisiana State University System, United States

****Correspondence:***
Agneta Andersson
agneta.andersson@umu.se

†Present address:
Joanna Paczkowska, Laboratorio de Oceanografía Biológica (LOBio), Centro para el Estudio de Sistemas Marinos (CESIMAR), Consejo Nacional de Investigaciones Científicas y Técnicas (CONICET), Puerto Madryn, Argentina
Owen Rowe, Baltic Marine Environment Protection Commission, Helsinki Commission (HELCOM), Helsinki, Finland
Robert Lefébure, ISEAL Alliance, London, United Kingdom

Specialty section:
This article was submitted to Marine Biogeochemistry, a section of the journal Frontiers in Marine Science

Received: *04 August 2019*
Accepted: *31 January 2020*
Published: *28 February 2020*

Citation:
Paczkowska J, Brugel S, Rowe O, Lefébure R, Brutemark A and Andersson A (2020) Response of Coastal Phytoplankton to High Inflows of Terrestrial Matter. Front. Mar. Sci. 7:80. doi: 10.3389/fmars.2020.00080

INTRODUCTION

Phytoplankton are the major primary producers in aquatic ecosystems (Field et al., 1998; Falkowski et al., 2004). They commonly constitute the base of pelagic food webs, thus changes in their taxonomic composition, size-structure and production due to anthropogenic activity and climate change can have complex and significant knock-on effects on the production at higher trophic levels (Chust et al., 2014; Rasconi et al., 2015). For example, periodically heavy rainfall will increase the transport of river-bond inorganic nutrients from the terrestrial system to the coast. The inorganic nutrient concentrations in the recipient waters will rise, which can promote phytoplankton growth (Dagg et al., 2004; Masotti et al., 2018). River flooding may therefore cause phytoplankton blooms and eutrophication in the recipient coastal ecosystems (Wasmund, 2002; Penna et al., 2004). However, if the river-water also holds high concentrations of colored humic rich matter, the eutrophication process could be counteracted (Andersson et al., 2013). The brownish color of the water causes increased light attenuation, and thus decreased water transparency. In such a scenario, phytoplankton growth would be light limited and their carbon production lowered. This may in turn lead to decreased fish production thus affecting human food resources.

Effects of river flooding on the coastal carbon cycle, induced by changes in the phytoplankton community, can vary (Roelke et al., 2013; Dorado et al., 2015). Increased inorganic nutrient levels would promote large microphytoplankton, such as diatoms (Shangguan et al., 2017a), since they have a competitive advantage when nutrient inputs are high (Legendre and Rassoulzadegan, 1995; Duarte et al., 2000). Furthermore, changes in the inorganic nutrient composition and their stoichiometry can drive the phytoplankton community to change the taxonomic composition and size-structure (Shangguan et al., 2017a,b; Swarbrick et al., 2019). On the other hand, low light levels would promote small phytoplankton, pico- and nanophytoplankton, because of their large surface to volume ratio and distribution of pigments along the outer cell wall (Raven, 1998; Marañón, 2015). This enables more efficient light harvesting in small cells compared to larger cells, where the light harvesting pigments are enclosed in inner cell organelles, i.e., in the chloroplasts (Raven, 1998; Kirk, 2011). However, since river water contains both inorganic nutrients and dissolved organic matter, freshwater inflows or flooding could either promote large or small phytoplankton cells. Moreover, where natural bacterial communities also make a significant part of the food web then the conversion of organic matter and the changes in bioavailability of it may also be critical factors (Asmala et al., 2013; Traving et al., 2017; Asmala et al., 2018). Thus overall, the phytoplankton response may be governed by the magnitude of the inflow and the inorganic nutrient and organic matter concentration in the river water.

Large and small phytoplankton cells can enter the food web, though this takes place at different trophic levels, implying that different shares of the organic carbon produced by phytoplankton reach higher trophic levels. At each trophic level, ∼70% of the energy (organic carbon) is lost due to respiration, sloppy feeding and excretion (Straile, 1997; Berglund et al., 2007). A simplified view is that the food web is size-structured and that the smallest picophytoplankton enter the food web at the flagellate level, while nanophytoplankton enter at the ciliate level and microphytoplankton at the mesozooplankton level (Legendre and Rassoulzadegan, 1995). This means that much less of the primary produced energy reaches higher trophic levels if the phytoplankton community is dominated by picophytoplankton than if the community is dominated by micro-sized phytoplankton (Sommer et al., 2002). In addition to that, there are quality differences between cyanobacteria and other phytoplankton groups (Peltomaa et al., 2017; Jónasdóttir, 2019). Cyanobacteria do not contain storage lipids, while many eukaryotic phytoplankton contain energy rich triacylglycerols (Nordbäck et al., 1998). All this emphasizes the need to understand how changing environmental conditions influence the composition, size-structure and productivity of the phytoplankton community.

To enable photosynthesis and growth at low light conditions phytoplankton often increase their content of light harvesting pigments, i.e., chlorophyll *a* (Markager, 1993; Dubinsky and Stambler, 2009). By this process phytoplankton may be able to maintain high primary production even though light levels and photosynthetic efficiency decrease (Halsey and Jones, 2015). However, with high terrestrial matter (tM) loading, the light may become too low to support primary production. Extreme inflows of tM may cause such a significant decrease in the under-water light conditions that a tipping point could be reached. Presently it is unknown how phytoplankton physiologically react to different loads of terrestrial matter. This is important to find out, since it gives a possibility to make ecological predictions of future climate change scenarios.

Changes in the phytoplankton community composition or size-structure can also be caused by zooplankton grazing under elevated tM loading conditions. Both increases and decreases of the zooplankton biomass have been found in tM-enrichment experiments, as well as alterations in the species composition (Carlsson et al., 1995; Berggren et al., 2010). Due to increased concentrations of nitrogen and phosphorus, intrinsic components of tM, primary production can be heightened, which can stimulate the zooplankton biomass (Klug, 2002; Kissman et al., 2013). Additionally, inorganic nutrients can regulate heterotrophic bacterial growth directly or indirectly via stimulation of autochthonous organic carbon production (Schweitzer and Simon, 1995; Vrede, 1999). On the other hand, if the light availability decreases due to the brown color of the tM, the primary production as well as the zooplankton biomass may decrease. Supply of tM however, also influences other food web components and can nurture the heterotrophic microbial food web, as the terrestrial organic carbon can be used as food source for heterotrophic bacteria (Kaartokallio et al., 2016). This in turn may promote growth of protozoa, which are used as food by mesozooplankton (Berggren et al., 2010; Faithfull et al., 2012). The bottom-up effects are major processes regulating the pelagic food web in oligotrophic ecosystems, while the top-down effects are more often observed in eutrophic ecosystems, where a positive correlation between mesozooplankton and picophytoplankton and heterotrophic bacteria occur due to

decreased predation pressure on small cells (a trophic cascade) (Sanders et al., 1992). Furthermore, phytoplankton are not always the most important food source for coastal zooplankton. For example, Carlsson et al. (1995) showed that zooplankton did not significantly influence the phytoplankton community in a coastal area, since the dominant omnivorous zooplankton rather grazed on microzooplankton than on phytoplankton. Additionally, tM may selectively alter the zooplankton species composition, and thus the food web channeling and stoichiometry (Berggren et al., 2010; Faithfull et al., 2012). Cladocerans have relatively low N:P ratio and execute unselective grazing (Hambright et al., 2007). They consume different organisms within the microbial food web, for example bacteria, flagellates and ciliates, and preferentially P-rich phytoplankton (Riemann, 1985; Schatz and McCauley, 2007). In contrast, copepods have a relatively high N:P ratio and are selective grazers (Meunier et al., 2016). They prefer feeding on nano- and microplankton, such as ciliates and N-rich phytoplankton species (Cowles et al., 1988; Walve and Larsson, 1999). The interaction between the food web-base and the mesozooplankton community is thus highly complex and adjustable depending on external forcing, for example varying inorganic nutrient and tM load.

Increasing inflows of tM to coastal areas in northern Europe, such as the Baltic Sea, is one of the projected consequences of future climate change (Meier et al., 2012; Andersson et al., 2015). Regional climate projections estimate an increase in riverine inflow of 15–20% in the northern Baltic Sea area, which will be accompanied by an increase in colored tM loads and inputs enriched with both organic and inorganic nutrients (Meier et al., 2012). We performed an experimental study to elucidate how projected increases in tM inflows will affect the coastal phytoplankton composition, size-structure, production and physiological adaptation. The experiment was performed using natural seawater from a coastal area in the northern Baltic Sea, which included a complete food web from microorganisms to mesozooplankton, with planktivorous fish subsequently added. We hypothesized that: (1) increased inorganic nutrient concentrations via tM inputs would cause an increase in the phytoplankton cell-size, even though the light decreases, (2) photosynthetic efficiency would decrease with increasing tM load and that the phytoplankton would adapt to lower light by increasing their chlorophyll *a* content, (3) at low tM load this adaptation would help maintaining high primary production rates but at high tM load high primary production cannot be sustained, and (4) mesozooplankton would benefit from high primary production, and their functional feeding composition would follow the size-spectrum of the phytoplankton community.

MATERIALS AND METHODS

Mesocosm Experiment

The experiment was carried out from 21st of May to 25th of June 2012, using 12 indoor mesocosms located at the Umeå Marine Sciences Center (UMSC), Sweden (as described in Traving et al., 2017). The mecososm are 5 m high tanks with a volume of 2000 l (see Grubisic et al., 2012; Lefébure et al., 2013 for more details). On May 21st and 22nd, seawater was gently collected at a depth of 4 m from the Bothnian Sea (63°33′N, 19°56′E; salinity ∼4 and temperature ∼6°C) using a peristaltic pump, and transported in 1 m^3 polythene containers to UMSC. Mesocosms were gently filled and enriched with inorganic nutrients (0.7 μmol l^{-1} nitrogen and 0.09 μmol l^{-1} phosphorus) to prevent nutrient limitation during a 7-day equilibration period prior to imposition of the treatments. The water contained a natural pelagic food web from bacteria to mesozooplankton, while larger organisms (e.g. fish) were excluded by using 1.5 mm mesh during collection. The final mesocosm temperature after a 7-day equilibration period reached 15°C and light was set to a cycle of 12 h light and 12 h dark. Illumination was supplied by 150 W metal halogen lamps (MASTERColour CDM-T 150W/942 G12 1CT) situated above each mesocosm, which provided photosynthetically active radiation (PAR) of 400 μmol photon m^{-2} s^{-1} at the surface. To ensure that the water column was replete with oxygen and well mixed, air was continuously bubbled into the mesocosms (20 ml s^{-1}) in conjunction with thermal cycling that resulted in convective stirring of the water (full mixing of each mesocosm in circa 2–4 h period, unpublished testing data).

Temperature and thermal water cycling within tanks was controlled by an automated heating/cooling system (±0.5°C). One of four treatments was assigned randomly to each mesocosm. Water exchange (40 l, inclusive of sampling water collection) was carried out every second day and replacement water consisted of 0.2 μm filtered natural Bothnian Sea water.

The experiment started on 28th of May (Day 0) and lasted for 28 days. To disentangle the effect of tM borne organic and inorganic nutrients, triplicate mesocosm replication was established. Four treatments were applied. In the tM_L and tM_H treatments, natural tM extracted from soils was added to mimic river inflow. The tM contained both organic matter and inorganic nutrients. Soils were collected at the beginning of May from the banks of the Reda River for tM_H (Southern Baltic Proper, Poland) and Öre River for tM_L (Northern Bothnian Sea, Sweden). The sites were selected to be representative of catchment regions dominated by agriculture and forestry, respectively. The tM extracts were produced following the procedure outlined in Lefébure et al. (2013). To release organic, inorganic nutrients and heavy metals bound to soils, extracts were dispersed in filtered MQ water and mixed with an ion exchange resin (Amberlite IRC 748I) before being stored in the dark at 4°C for 48 h. Extracts were then filtered through a 90 μm mesh and the liquid phase was retained in acid washed tanks in the dark at 4°C for the duration of the experiment. Nutrient (inorganic and total) measurements of these extracts were made on filtered samples from the bulk extracts, and this information was used to create the treatments described below. Dissolved organic carbon (DOC), dissolved inorganic nitrogen and phosphorus (DIN, DIP), total nitrogen and phosphorus (Tot N, Tot P) concentrations were analyzed using a Shimadzu TOC-5000 carbon analyzer and a Braan and Luebbe TRAACS 800 autoanalyzer. The experiment was designed to mimic a future climate change scenario of increased river runoff in the Baltic Sea. The final concentration of DOC targeted was 6 mg l^{-1} in the tM_L treatment and 8 mg l^{-1}

in the tM_H treatment (overall additions), which is equivalent to an increased C concentration of 50 and 100% respectively, based on future scenario from Hägg et al. (2010). The two control treatments $Ctrl_L$ and $Ctrl_H$ were supplemented only with inorganic N and P to match inorganic nutrients concentrations of the respective tM treatments. Three days before the first sampling day, all mesocosms were supplied with a 22% boost of their respective overall additions, followed by daily equal additions to reach future C scenarios (**Table 1**). During the first day of the experiment (Day 0), seven young of the year (YOY), similarly sized, perch (*Perca fluviatilis*) were added per mesocosm to mimic natural predation. The fish survival during the experiment was high, with an average survival rate of 80%.

Sampling

All water samples were collected twice a week in the early morning (06.00 h) using a syphoning hose at 2 m depth, except those for microscopic identification of phytoplankton and zooplankton. These samples were taken at the beginning, middle and end of the experiment (Days 0, 17, and 28) using the same sampling device. Primary production incubation was performed immediately after sample collection and once the automatic light cycle had been initiated (07.00 h).

Physicochemical Factors

Vertical Photosynthetically Active Radiation (PAR) irradiance profiles were taken with a LICOR-193SA light sensor. Light measurements were carried out every 0.2 m from the surface to 0.6 m, and then at 0.5 m intervals down to 4.5 m. The light attenuation coefficient (K_d) was calculated from the slope of the linear regression of the natural logarithm of downwelling irradiance versus depth. Samples for inorganic nutrients Dissolved Inorganic Phosphorus (DIP: phosphate), Dissolved Inorganic Nitrogen (DIN: nitrate + nitrite and ammonium) and silicate were filtered through 0.2 μm cellulose-acetate filters and stored at −20°C, while unfiltered samples for total phosphorus (Tot P) and total nitrogen (Tot N) were directly stored at −20°C. All nutrients were analyzed using a Braan and Luebbe TRAACS 800 autoanalyzer, according to standard analytical methods (Grasshoff et al., 1983). The concentration of humic substances (HS) was measured from unfiltered water samples using a Perkin Elmer LS 30 fluorometer at 350/450 nm excitation/emission wavelengths, calibrated with a serial dilution of quinine sulfate solution (Hoge et al., 1993). DOC concentrations were analyzed on 0.22 μm filtered (Supor Membrane Syringe Filter, non-pyrogenic; Acrodisc®) and acidified samples (18 mM HCl, final concentration) using a Shimadzu TOC-5000 analyzer.

Colored dissolved organic matter (CDOM) absorbance was measured in water samples filtered through a 0.22 μm polycarbonate membrane and stored in amber glass bottles in the dark at 4°C until analysis. Absorbance values were recorded from 250 to 800 nm using a Shimadzu UVPC-2501 scanning spectrophotometer, with Milli-Q water as the blank. The absorption coefficient at 440 nm (g_{440}) was calculated by multiplying the absorbance at specific wavelength with 2.303 and dividing by the length of the cuvette (Kirk, 2011).

TABLE 1 | Daily addition of C, N and P concentrations in the mesocosms (subsequent to initial addition of tM extracts).

Treatment	C (μmol l^{-1})	N (μmol l^{-1})	P (μmol l^{-1})
tM_L*	10	1.1	0.03
tM_H*	20	2.3	0.13
$Ctrl_L$**	–	0.001	0.0008
$Ctrl_H$**	–	0.009	0.005

**Soil extracts contained both organic and inorganic nutrients as well as dissolved organic carbon. **$Ctrl_L$ and $Ctrl_H$ treatments were supplemented with nitrate ($NaNO_3$), ammonia (NH_4Cl) and phosphate (NaH_2PO_4) in the stoichiometry and concentration equivalent to tM addition treatments, respectively [from Traving et al. (2017)].*

Chlorophyll *a* and Primary Production

Samples for chlorophyll *a* (Chl *a*) (100 ml) were filtered onto 25 mm GF/F filters, extracted in 95% ethanol overnight and measured with a Perkin Elmer LS 30 fluorometer (433/674 nm excitation/emission wavelengths). Primary production (PP) rates were measured using the ^{14}C method (Gargas, 1975). Samples were incubated with $NaH^{14}CO_3$ at a final concentration of 0.1 μCi ml^{-1} (^{14}C Centralen Denmark, DHI, activity 100 μCi ml^{-1}) at seven depths: surface, 0.1, 0.2, 0.4, 0.6, 1, and 2 meters, within each mesocosm. Additionally, one dark sample per tank was incubated. After ∼3 h of incubation, 5 ml of each sample were transferred to a scintillation vial, and gently bubbled with 150 μl of 6 M HCl for 30 min. Subsequently, 15 ml of scintillation fluid were added, and samples were measured using a Beckman 6500 scintillation counter. Average daily primary production was calculated in each mesocosm, using the light factor method (Gargas, 1975). PP:Chl *a* was calculated as an indicator of photosynthetic efficiency.

Bacterial Production

The ^3H-thymidine incorporation method was used to measure bacterial production (BP) (Fuhrman and Azam, 1982). Four 1 ml seawater samples (one control and three samples) were incubated with 2 μl of ^3H-thymidine (84 Ci $mmol^{-1}$; PerkinElmer, MA, United States) (final concentration 24 nM) for 1 h at *in situ* temperature. This thymidine addition corresponded to the saturation level. The control sample was pre-killed by adding 100 μl of ice-cold 50% TCA and incubation at −20°C for 5 min. Cell production was calculated using a conversion factor of 1.4×10^{18} cells mol^{-1} of incorporated thymidine (Wikner and Hagström, 1999). Daily net production rates were calculated assuming stable uptake rates over the day and a bacterial carbon content of 20 fgC $cell^{-1}$ (Lee and Fuhrman, 1987).

Plankton Identification and Enumeration

Samples for phytoplankton (>2 μm) identification and counting were preserved with 2% alkaline Lugol's solution in 50 ml volumes. Samples were settled for 24–48 h and counted using the inverted microscope method (Utermöhl, 1958). Microphytoplankton (>20 μm) and nanophytoplankton (2–20 μm) samples were counted at 100× and 400× magnification, respectively. Zooplankton samples were preserved with 2%

alkaline Lugol's solution, counted on a stereomicroscope (Leica), and transformed into carbon biomass (Hernroth, 1985).

Samples for picophytoplankton and heterotrophic bacteria were preserved in 0.1% glutaraldehyde (final concentration) and frozen at −80°C (Marie et al., 2005) for later counts using a BD FACSVerse™ flow cytometer (BD Biosciences) equipped with a 488 nm laser (20 mW output) and a 640 mn laser (output 40 mW). Frozen samples were quickly thawed in a 30°C water bath and pre-filtered through a 50 μm mesh. Picophytoplankton samples were run with 3 μm microspheres (Fluoresbrite® plain YG, Polysciences) as internal standard. Picophytoplankton abundance was converted to biomass using carbon conversion factors: 120 fgC cell^{-1} for picocyanobacteria and 829 fgC cell^{-1} for picoeukaryotic phytoplankton, based on microscopic measurements of cell sizes and use of conversion factors (see below). Heterotrophic bacteria samples were diluted with 0.2 μm filtered seawater, stained with SYBR Green I (Invitrogen) (1:10000, final concentration) and kept in the dark at room temperature for 10 min. 1 μm microspheres (Fluoresbrite® plain YG, Polysciences) were added to each sample as internal standard and analyses were run at a low flow rate of 30 μL min^{-1} with an acquisition time of 2 min. Heterotrophic bacteria abundance was converted to biomass using carbon conversion factor: 20 fgC cell^{-1} (Lee and Fuhrman, 1987).

The phytoplankton cells were divided into different size-classes: pico- (<2 μm), nano- (2–20 μm), and micro- (>20 μm) phytoplankton based on measurements of the longest cell axis. Functional groups: AU (autotrophs), HT (heterotrophs), and MX (mixotrophs) were assigned according to Olenina et al. (2006). Filamentous cyanobacteria were assigned to the microphytoplankton category based on the size of single cells, as well as tightly clustered amalgamations of cells. Nutritional characteristics of plankton were identified based on cell morphology, size and described trophy (Tikkanen and Willen, 1992; Hällfors, 2004; Olenina et al., 2006). Further, the coloration of the smallest cells was used to support the trophy classification as Lugol's solution stains Chl *a* brown. Phytoplankton biomass was calculated from the geometric shape of cells following Olenina et al. (2006) and cell carbon content was calculated according to Menden-Deuer and Lessard (2000). Total phytoplankton biomass (TB) was defined as the sum of the carbon biomass of autotrophs (including *Mesodinium rubrum*) and mixotrophs. The relative contribution to biomass of size classes and functional groups were calculated. Additionally, Chl *a*:C was estimated as an indicator of acclimation to changing light and nutrient conditions. This indicator was obtained by dividing the Chl *a* concentration by total phytoplankton carbon biomass.

Statistical Analyses

Generalized linear mixed models (GLMM), followed by Tukey's *post hoc* tests, were used to test the effect of treatments, days and their interactions on physicochemical variables and biological variables. Mesocosm tank was included as a random effect. The assumptions of normality were tested using the Shapiro-Wilk test. The fit of the model was estimated by interpreting the diagnostic plots (correlation between model residuals and the fitted values, normality of residuals, homoscedasticity of the residuals and possible data outliers). GLMM models were also performed to evaluate the effects of physicochemical and biological variables (PAR, PO_4, NH_4, $NO_3 + NO_2$, and zooplankton biomass) on phytoplankton related parameters, bacterial biomass and production and ciliate biomass. The remaining physicochemical variables measured during the experiment were not included in analysis due to high multicollinearity indicated by the variance inflation factor (VIP > 10). Physicochemical and biological variables were selected for the final model with a backward stepwise selection process based on based on Akaike's Information Criterion (AIC). Changes in the total phytoplankton biomass composition were visualized by non-metric multidimensional scaling (NMDS), based on Bray-Curtis similarity. Redundancy analysis (RDA) was performed to identify factors influencing the size-structure of the phytoplankton community during the middle and end of the experiment. The relative biomass of pico- (<2 μm), nano- (2–20 μm) and micro- (>20 μm) phytoplankton were analyzed in relation to zooplankton biomass (Zooplankton), phosphate (PO_4), ammonium (NH_4), nitrate + nitrite ($NO_3 + NO_2$), and Photosynthetically Active Radiation (PAR). Additionally, the relationships between primary production (PP), bacterial production (BP), zooplankton biomass (ZP), and ciliate biomass (Ci) as endogenous variables and phosphate (PO_4) and dissolved organic carbon (DOC) as exogenous variables were examined by structural equation modeling (SEM). Standardized path coefficients and R^2 were calculated, while the goodness of fit of the model was tested by the Chi-square test. Non-parametric correlation (Spearman) analyses were used to test relationships between the relative biomass of major zooplankton groups and bacterial, ciliate biomass and the relative contribution of the size-structure of the phytoplankton. Day 0 was excluded from statistical analyses in order to examine physicochemical and biological variations after the treatments had taken effect. Data analyses were performed in Primer 6, Canoco 5, and R softwares.

RESULTS

Variation of Physicochemical Factors

Photosynthetically Active Radiation (PAR) decreased gradually over time in the mesocosms with tM load (33–4 μmol photon m^{-2} s^{-1}), while in the controls ($Ctrl_L$ and $Ctrl_H$) the PAR values were higher and generally more constant (on average 50 μmol photon m^{-2} s^{-1}) (Tukey's, $p < 0.001$) (**Figure 1A**). Humic substances, K_d, Tot N, DOC and g_{440} increased throughout the experiment in the tM mesocosms (HS: 26–47 μg l^{-1}, K_d: 1.4–4.1 m^{-1}, Tot N: 22–40 μmol^{-1}, DOC: 6-9 mg l^{-1}, g_{440}: 2.6-9.7 m^{-1}), while in the controls the values were relatively unchanged (on average HS: 22 μg l^{-1}, Kd: 1 m^{-1}, Tot N: 17 μmol^{-1}, DOC: 5 mg l^{-1}, g440: 1.7 m^{-1}) (**Figures 1B**, **2A,C–E**). The values of these variables were significantly higher in the tM supplemented mesocosms compared to the controls (Tukey's, $p < 0.001$).

In general, nitrate + nitrite decreased steadily over time in all treatments and reached the lowest values on day 24 (**Figure 1C**).

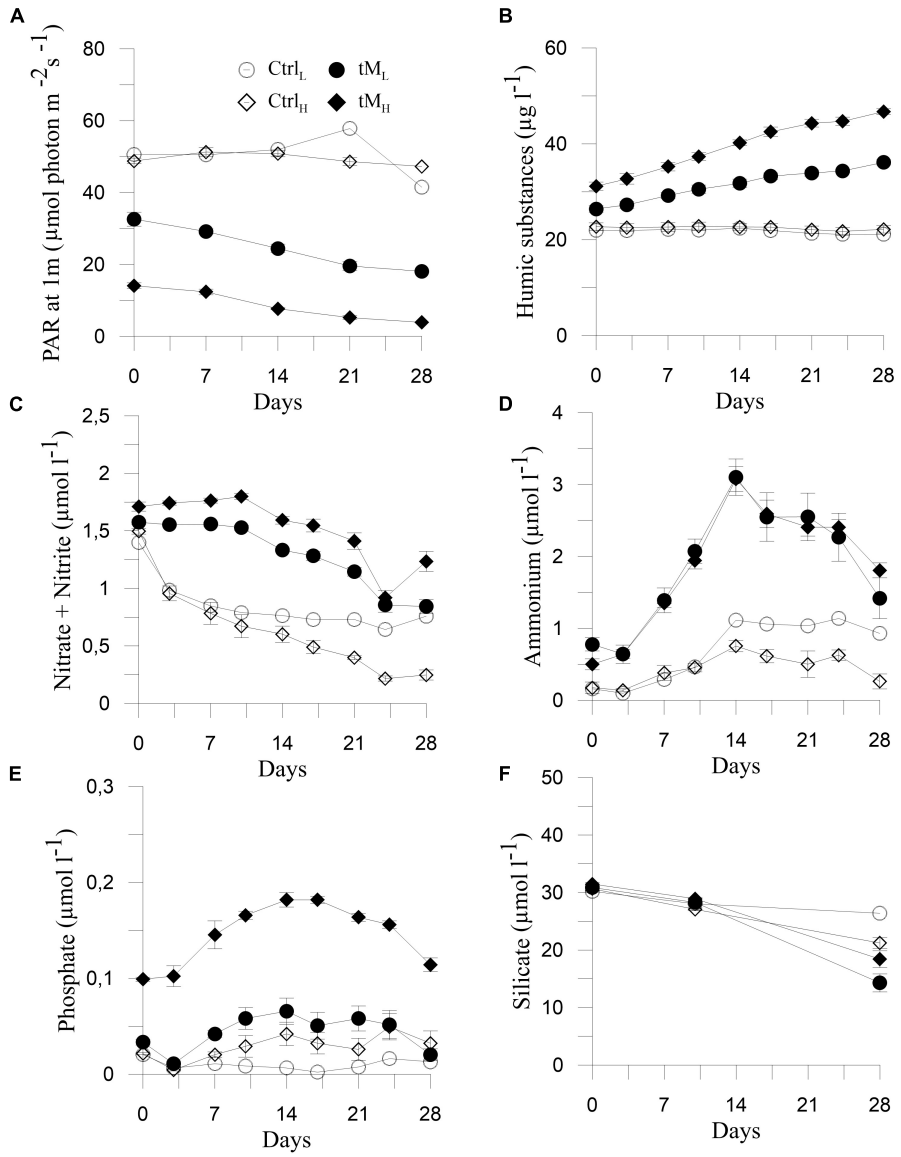

FIGURE 1 | Temporal variation of physicochemical factors during the experiment: Photosynthetic Active Radiation (PAR) at 1 m **(A)** modified after Traving et al. (2017), humic substances **(B)**, nitrate + nitrite **(C)**, ammonium **(D)**, phosphate **(E)**, and silicate **(F)**. Means ± standard error, $n = 3$.

Higher nitrate + nitrite concentration was observed in tM treatments than in controls (1.4 ± 0.1 vs. 0.8 ± 0.1 µmol l^{-1}). Ammonium, phosphate and Tot P peaked at the middle of the experiment, reaching maximum values in tM treatment (3.1 µmol^{-1} for ammonium, 0.18 µmol^{-1} for phosphate and 0.83 µmol^{-1} for Tot P, respectively) (**Figures 1D,E**, **2B**). Inorganic nitrogen (nitrate + nitrite and ammonium), phosphate and Tot P concentrations were significantly higher in the tM mesocosms than in the controls (Tukey's, $p < 0.001$). The higher concentrations of inorganic N and P in the tM treatments than in the controls were likely due to bacterial reduction of organic N and P to inorganic forms. Silicate showed a decreasing trend in all mesocosms, and at the end of the experiment, the silicate concentration was 1.5-fold lower in the tM mesocosms than in the controls (16.4 ± 2.1 vs. 23.8 ± 2.6 µmol^{-1}) (**Figure 1F**). There was no significant difference in silicate concentration between treatments. Highest DIN:DIP ratio was observed in the control ($Ctrl_L$). In these mesocosms the ratio was 2-fold and 8-fold higher than in the remaining treatments, suggesting strong phosphorus limitation in $Ctrl_L$ (**Figure 2F**).

Effect of tM Load on Phytoplankton Community Composition, Size-Structure and Nutritional Strategy

The taxonomic composition was similar in all mesocosms at the beginning of the experiment (**Figures 3A**, **4**). Bacillariophyceae and Chlorophyceae were the dominant groups (**Figures 3Aa-d**).

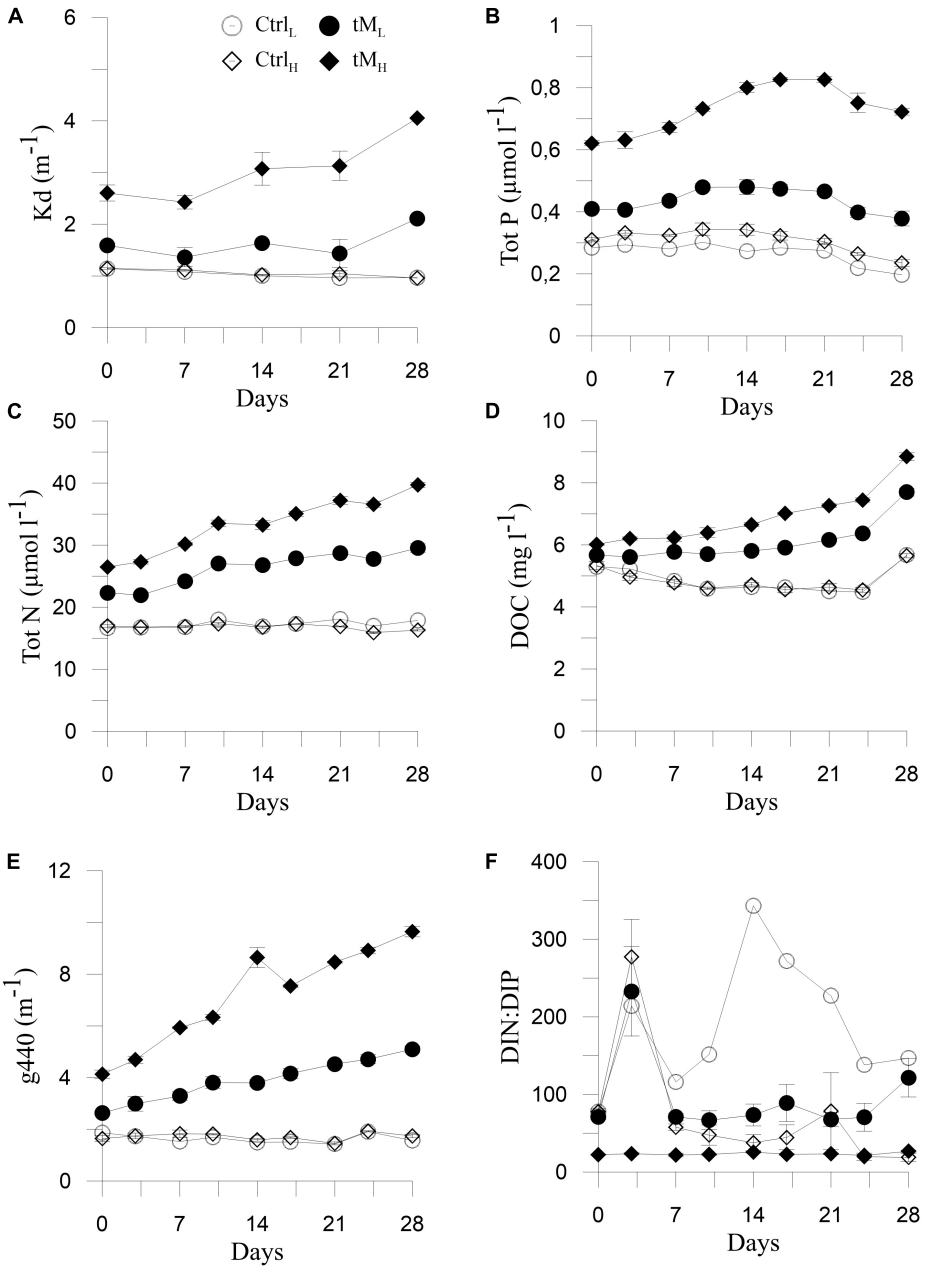

FIGURE 2 | Temporal variation of physiochemical factors: Kd **(A)**, Tot P **(B)**, Tot N **(C)**, DOC **(D)** modified after Traving et al. (2017), g440 **(E)**, and DIN:DIP **(F)**. Mean ± standard error, $n = 3$.

Noticeable taxa were *Skeletonema marinoi* (Cleve), *Thalassiosira baltica, Chaetoceros wighamii* (Brightwell) and *Monoraphidium contortum* (Komárková-Legnerová). The photosynthetic ciliate *Mesodinium rubrum* (Leegaard) also occurred abundantly at the initial phase of the experiment, constituting on average ∼10% of the total biomass in controls and ∼25% in tM treatments (**Figures 3Aa-d**). However, as the experiment progressed the phytoplankton composition showed differences between the controls and tM supplemented mesocosms (**Figures 3A**, **4**). In the controls, unidentified picoeukaryotes dominated the phytoplankton community (**Table 2** and **Figures 3Aa-b**), while in the tM supplemented mesocosms they constituted a smaller share (**Figures 3Ac-d**). Bacillariophyceae (diatoms) were promoted by tM load, and at the end of the experiment this group constituted on average ∼50% of the biomass in these mesocosms (**Figures 3Ac-d**). *Diatoma tenuis* (C. Agardh) and *Synedra acus* var. *acus* (Kützing) were the most abundantly occurring species.

At the start of the experiment, microphytoplankton was the dominant size group in all mesocosms, forming ∼80%

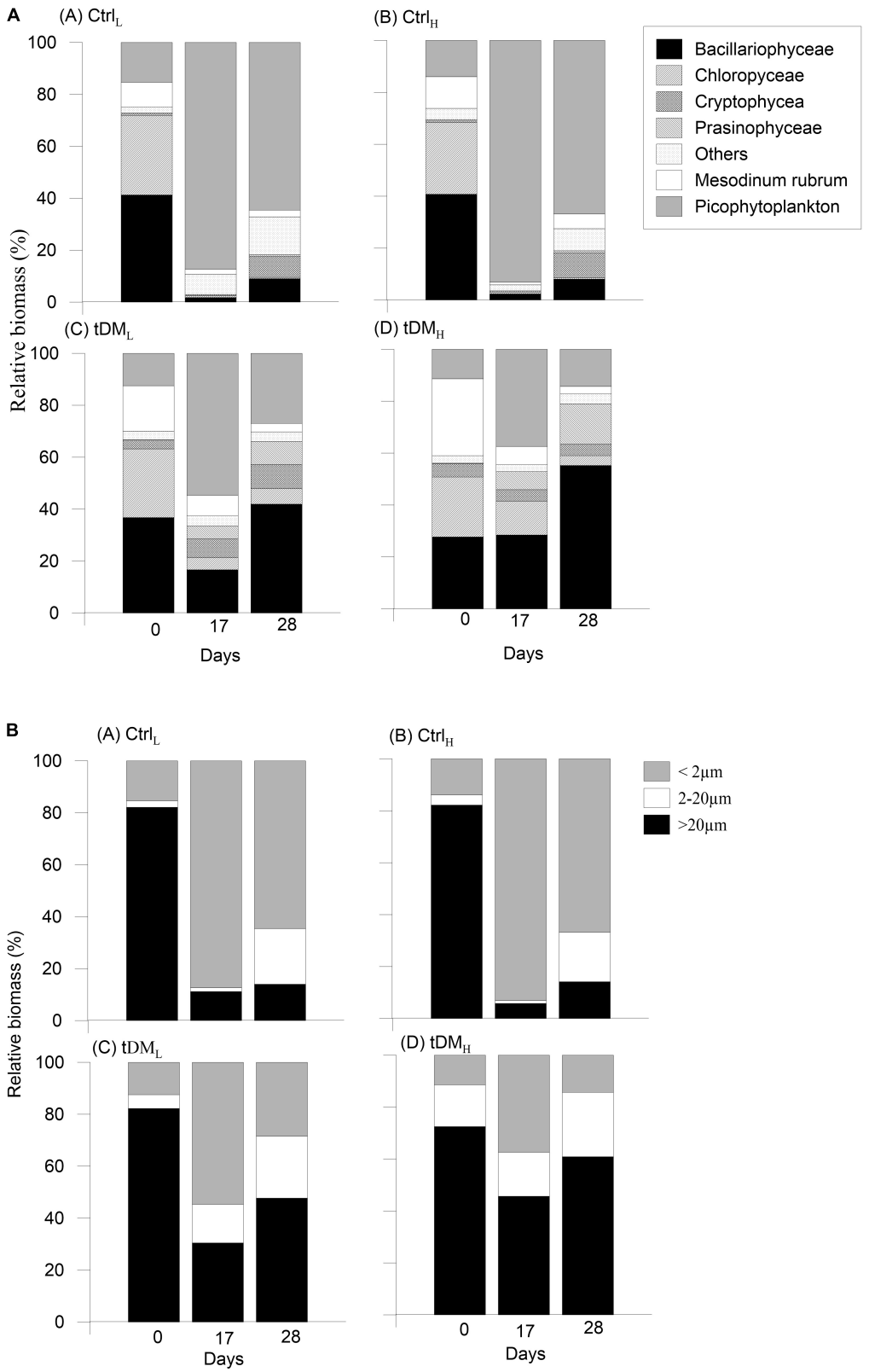

FIGURE 3 | Phytoplankton taxonomic composition and size-structure at the start, middle and end of the experiment: biomass distribution of major phytoplankton taxa: Bacillariophyceae, Chlorophyceae, Cryptophyceae, Prasinophyceae, Others, Mesodinum rubrum and picophytoplankton **(A)**, and biomass distribution of size-classes: pico- (<2 μm), nano- (2–20 μm), and microphytoplankton (>20 μm) **(B)**.

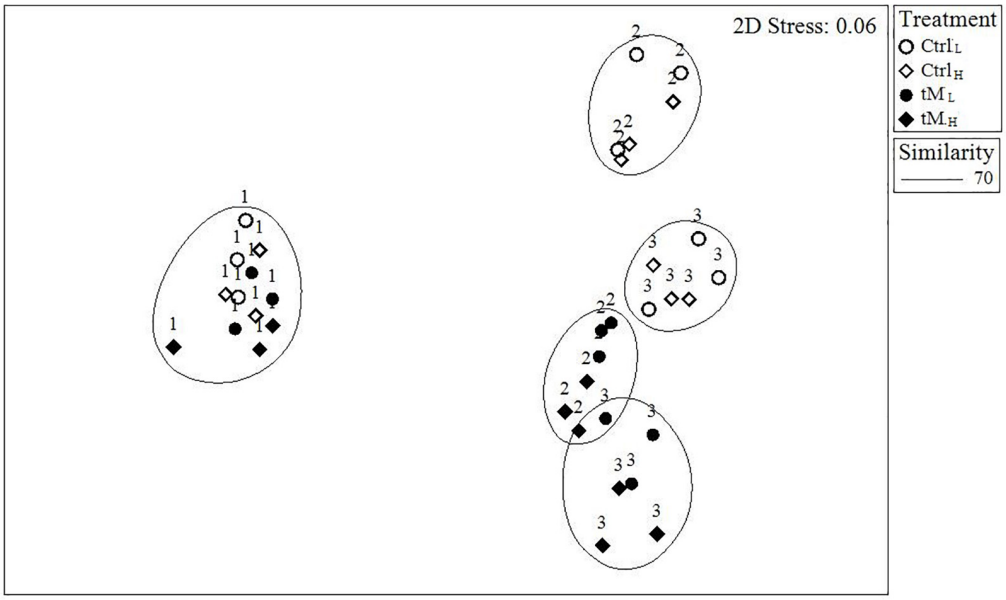

FIGURE 4 | Non-metric multidimensional scaling (NMDS) plot of the phytoplankton community composition. Numbers display the sampling day (1 = Day 0, 2 = Day 17, and 3 = Day 28).

of the biomass (**Figures 3Ba-d**). Their relative contribution decreased most strongly in the controls, falling to less than 10% in the middle of the experiment before increasing slightly by the end of the experiment, reaching ∼14%. In the tM supplemented mesocosms, the microphytoplankton contribution remained high throughout the experiment and ranging between 31 and 46% in the middle of the experiment and 48 and 61% at the end of the experiment. *D. tenuis*, *M. rubrum*, *S. acus* var. *acus* and *M. contortum* dominated this phytoplankton size group over the experiment (**Table 2**). Nanophytoplankton constituted a smaller part of the phytoplankton community, on average ∼1% of the total phytoplankton biomass in the controls and ∼15% in tM treatments in the middle of the experiment, while the highest share, ∼25%, was observed at the end of the experiment in all treatments (**Figures 3Ba-d**). Within the nanophytoplankton, Cryptophyceae and Prasinophyceae were the most abundant taxa, e.g., *Plagioselmis prolonga* (Butcher), *Teleaulax* spp. and *Pyramimonas* spp. (**Table 2**). Picophytoplankton showed maximum contribution in the middle of the experiment in all mesocosms, where they constituted 38–93% of the phytoplankton biomass (**Figures 3Ba-d**). The picophytoplankton share remained high in the controls all through the experiment, while in the tM mesocosms picophytoplankton decreased toward the end, constituting ∼20% of the phytoplankton biomass (**Figures 3Ba-d**).

The proportion of autotroph biomass was high in all treatments, constituting over 96% of the total phytoplankton biomass throughout the experiment. The contribution of heterotrophs and mixotrophs was minimal, contributing a maximum of ∼4% in the tM mesocosms in the middle of the experiment, and 2% in controls at the end of the experiment.

Relation Between Phytoplankton Size-Structure and Potentially Explanatory Factors

The influence of environmental conditions on the size-structure of the phytoplankton community was explored using Redundancy analyses (RDA). The first two RDA axes explained 83.6% of the phytoplankton size-structure (**Table 3**). RDA1 was mainly influenced by PAR and zooplankton biomass, and RDA2 had high scores of zooplankton biomass and inorganic nitrogen forms (nitrate + nitrite) (**Figure 5**). The environmental conditions within the controls contributed to higher relative contributions of picophytoplankton and zooplankton biomass, while microphytoplankton dominated in the tM enriched mesocosms, where PAR was low and inorganic nutrients high.

Chlorophyll *a*, Total Phytoplankton Biomass and Chlorophyll *a* Content

In the controls the Chl *a* and total phytoplankton biomass showed an overall decreasing trend over time, with values that were 2–4 times lower at the end of the experiment than at the start (**Figures 6A,B**). In the tM enriched mesocosms, Chl *a* and total phytoplankton biomass decreased until the middle of the experiment and then slightly increased toward the end of the experiment (**Figures 6A,B**). The Chl *a* concentrations and total phytoplankton biomass were significantly lower in the tM_H mesocosms compared to the other treatments (Tukey's, $p < 0.05$). During the second part of the experiment the average Chl *a* and total phytoplankton biomass were the lowest in the tM_H mesocosms (∼1.1 μg l^{-1} and ∼15 μg C l^{-1}, respectively) (**Figures 7A,B**). Chl *a* concentration was positively

TABLE 2 | Dominating phytoplankton taxa, constituting >25% of the biomass in different size classes, at day 17 and 28 of the mesocosm experiment.

Size fraction	$Ctrl_L$		$Ctrl_H$		tM_L		tM_H	
	Day 17	Day 28	Day 17	Day 28	Day 17	Day 28	Day 17	Day 28
<2 µm	Picoeukaryotes	Picoeukaryotes	Picoeukaryotes	Picoeukaryotes	Picoeukaryotes	Picoeukaryotes	Picoeukaryotes	Picoeukaryotes
2–20 µm	Centrales unidentified *Plagioselmis prolonga*	*Pseudopedinella tricostata*	*Plagioselmis prolonga*	*Teleaulax* spp.	*Plagioselmis prolonga* *Pyramimonas* spp.	*Pyramimonas* spp. *Teleaulax* spp.	*Pyramimonas* spp.	*Pyramimonas* spp.
>20 µm	*Merismopedia warmingiana*	*Diatoma tenuis*	*Diatoma tenuis* *Merismopedia warmingiana*	*Mesodinium rubrum*	*Diatoma tenuis* *Mesodinium rubrum*	*Diatoma tenuis* *Synedra acus* var. *acus*	*Diatoma tenuis* *Monoraphidium contortum*	*Diatoma tenuis* *Synedra acus* var. *acus*

TABLE 3 | Variable loadings for the first and second axis of the RDA performed on biological and physicochemical data.

	Axis	
	1	2
Eigenvalues	0.811	0.025
Pseudo-canonical correlations	0.941	0.550
Cumulative percentage variance		
of response data	81.1	83.6
of fitted response data	96.9	99.9
Variables:		
Photosynthetically Active Radiation (PAR)	−0.862	0.132
Zooplankton	−0.761	−0.284
Nitrate + nitrite ($NO_3 + NO_2$)	0.545	−0.278
Phosphate (PO_4)	0.498	−0.110
Ammonium (NH_4)	0.486	−0.233

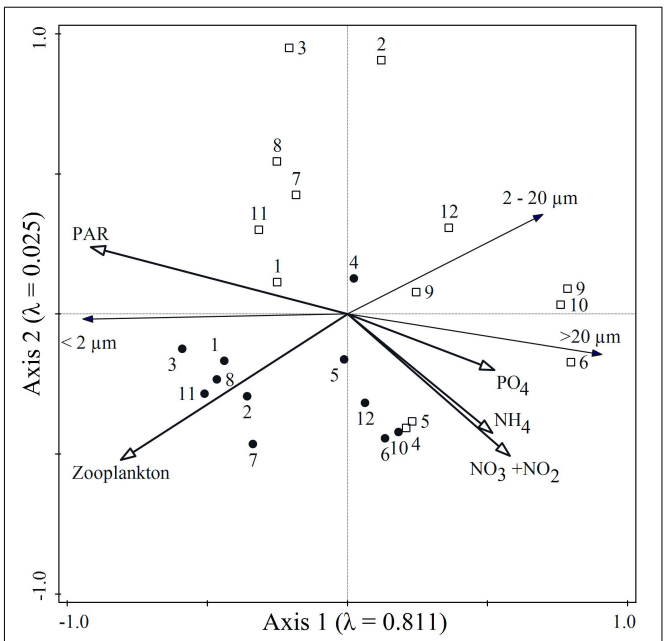

FIGURE 5 | Redundancy analysis (RDA) of factors influencing the size-structure of the phytoplankton community during the middle and end of the experiment. The distribution of pico- (<2 µm), nano- (2–20 µm) and micro- (>20 µm) phytoplankton were analyzed in relation to zooplankton biomass (Zooplankton), phosphate (PO_4), ammonium (NH_4), nitrate + nitrite ($NO_3 + NO_2$) and Photosynthetically Active Radiation (PAR). Numbers display mesocosm numbers (Ctr_L (1,2,7), Ctr_H (3,8,11), tM_L (4,5,12), tM_H (6,9,10), ●- Day 17; □ – Day 28).

correlated with ammonium while total phytoplankton biomass was negatively correlated with phosphorus (**Supplementary Table S1**). The Chl *a* content of the phytoplankton cells, measured as the Chl *a*:C ratio, was on average about 50% higher in the tM supplemented mesocosms than in the controls, largely due to increase phosphorus concentrations (**Figure 7C** and **Supplementary Table S1**).

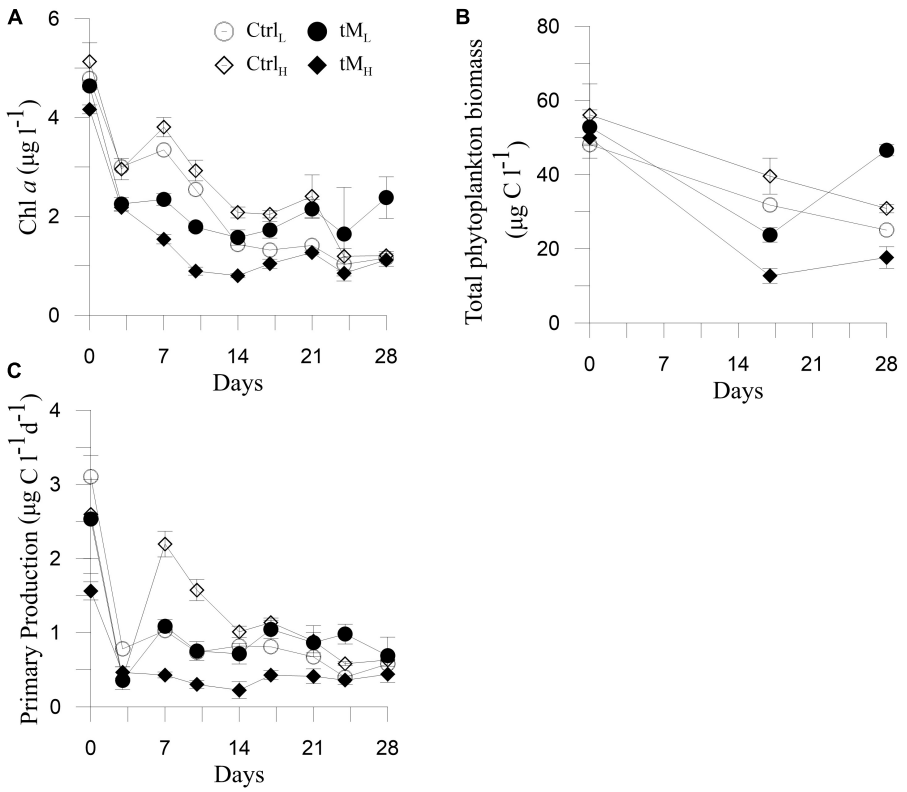

FIGURE 6 | Temporal variation of Chl *a* **(A)** modified from Traving et al. (2017), total phytoplankton biomass **(B)** and primary production **(C)**. Means ± standard error, $n = 3$.

Variation of Phytoplankton Primary Production and Photosynthetic Efficiency

Primary production ranged from 0.2 to 3.1 µg C l^{-1} d^{-1} during the experiment (**Figure 6C**). In the tM enriched mesocosms, primary production was significantly lower than in the controls (**Figures 6C**, **7D**) (Tukey's, $p < 0.01$). When the different treatments had taken effect, i.e., during the second half of the experiment, the low tM enrichment (tM$_L$) showed a positive effect on primary production compared to the control (Ctrl$_L$) (**Figure 7D**). In fact, the primary production was similar in the control (Ctrl$_H$) and tM enriched mesocosms (tM$_L$), while in the tM$_H$ mesocosms the primary production was approximately half of that in the other treatments (**Figure 7D**). The photosynthetic efficiency, i.e., the PP:Chl *a* ratio was higher in the controls than in the tM supplemented mesocosms (0.57 ± 0.03 vs. 0.43 ± 0.02) (**Figure 7E**). PP and PP:Chl *a* ratio were negatively correlated with phosphate and positively with zooplankton biomass and ammonium (**Supplementary Table S1**).

Bacterial Biomass and Productivity

Bacterial biomass generally increased until the middle of the experiment in all treatments after which it sharply declined (**Figure 8A**). A significantly higher bacterial biomass was observed in tM$_L$ than tM$_H$ mesocosms (77.5 ± 7.0 vs. 64.8 ± 3.8 µg l^{-1}) (Tukey's, $p < 0.001$). Bacterial production ranged between 0.44 and 2.78 µg C l^{-1} d^{-1} and was on average 1.5 times lower in the Ctrl$_H$ treatment compared to the remaining treatments, with relatively stable values throughout the experiment (**Figure 8B**). In both tM treatments, bacterial production followed a similar trend as bacterial biomass (**Figure 8B**). Bacterial production in tM$_H$ was significantly higher than in Ctrl$_H$ (Tukey's, $p < 0.01$). During the second part of the experiment, higher bacterial production was observed in tM addition treatments than in controls (**Figure 7F**). Bacterial biomass was positively correlated with zooplankton biomass and nitrate + nitrite concentration while bacterial production with ammonium (**Supplementary Table S1**).

Ciliates and Mesozooplankton Biomass

The ciliate biomass, which initially was 0.08 and 0.14 µg C l^{-1} in controls and tM mesocosms, slightly decreased in the middle of the experiment and then decreased to 0.04 and increased to 0.35 µg C l^{-1} by the end of the experiment, respectively (**Figure 8C**). A significant difference between tM treatments and their controls was observed (Tukey's, $p < 0.01$). Ciliate biomass was negatively correlated with phosphate, PAR and ammonium (**Supplementary Table S1**). Mesozooplankton biomass increased from the start to the middle of the experiment and then decreased toward the end of the experiment. Higher mesozooplankton

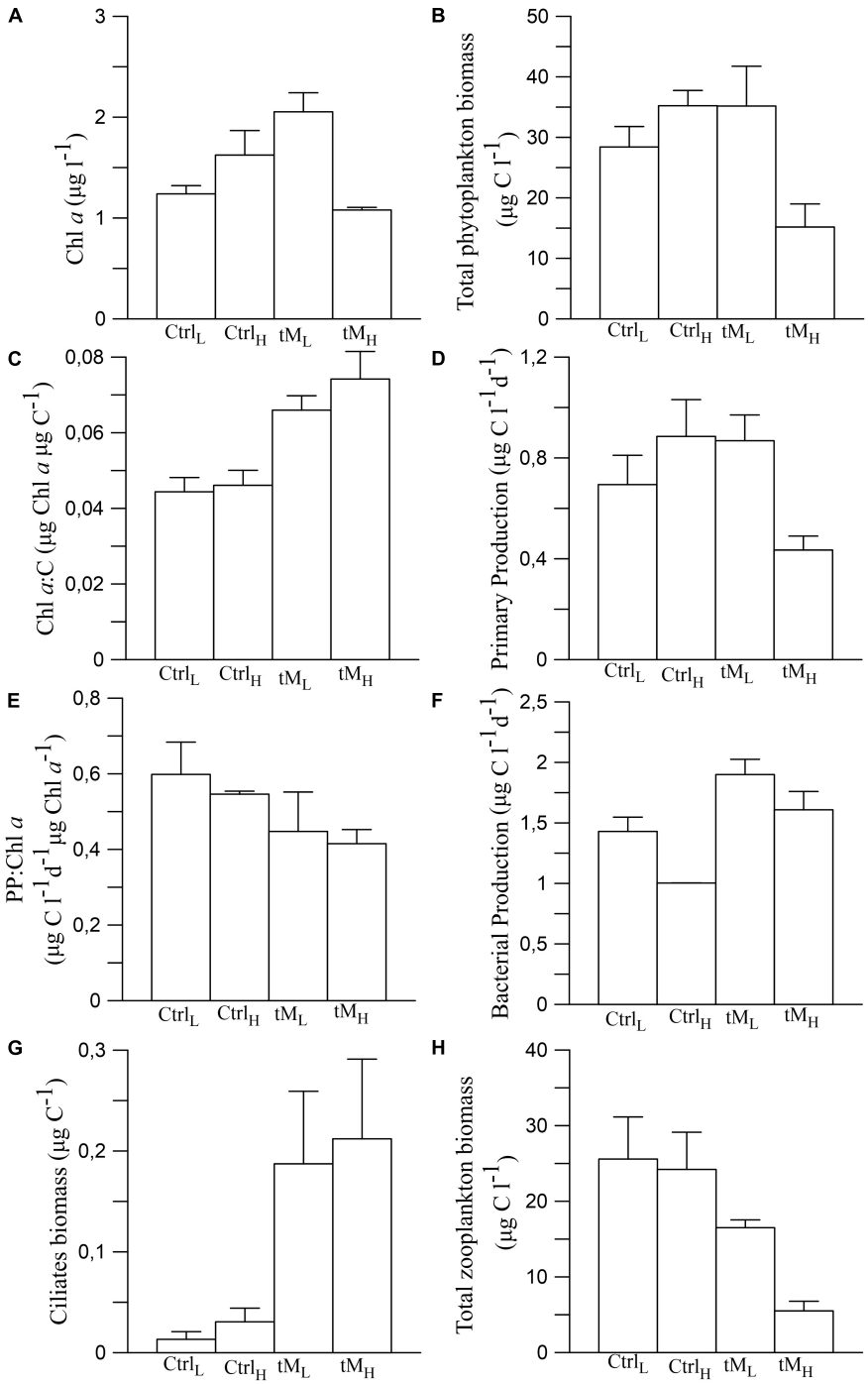

FIGURE 7 | Average Chl *a* **(A)**, total phytoplankton biomass **(B)**, Chl *a*:C **(C)**, primary production **(D)**, PP:Chl *a* **(E)**, bacterial production **(F)**, ciliate biomass **(G)**, and the zooplankton biomass **(H)** during the second part of the experiment (Day 17 and Day 28). Means ± standard error, $n = 2$.

biomass was observed in the controls than in tM treatments (19.7 ± 2.6 vs. 11.7 ± 1.6 µg C l^{-1}) (**Figure 8D**) (Tukey's, $p < 0.01$). During the second part of the experiment, ciliate biomass was higher in tM addition mesocosms, while the opposite trend was observed in relation to the zooplankton biomass (**Figures 7G,H**). Structural equation modeling (SEM) showed that DOC promoted the ciliate biomass (standardized path coefficient 0.74, $p < 0.05$), and was negatively correlated with primary production and zooplankton biomass (standardized path coefficient −0.41 and −0.75, $p < 0.05$, respectively) (**Figure 9**). The model indicated that DOC hampered the bacterial production, and that bacterial and primary production were positively correlated. Overall, the

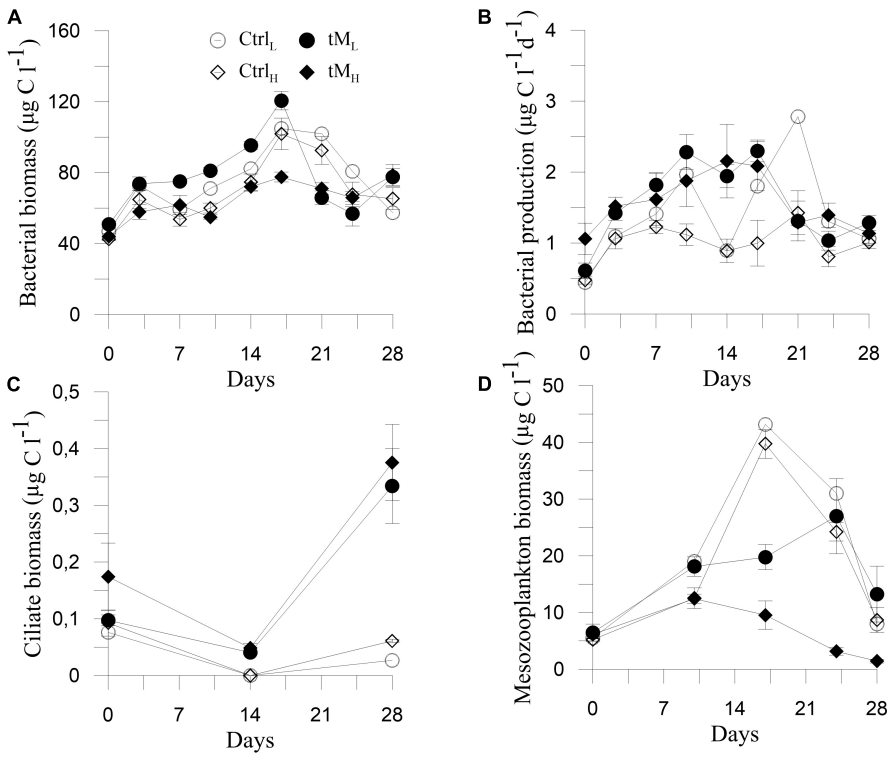

FIGURE 8 | Temporal variation of bacterial biomass **(A)**, bacterial production **(B)**, ciliate biomass **(C),** and mesozooplankton biomass **(D)**. Means ± standard error, $n = 3$.

SEM model showed a similar goodness of fit to the data ($\chi^2 = 0.40$, $df = 2$, $p = 0.82$).

Mesozooplankton Community Composition

At the beginning of the experiment the zooplankton community was dominated by *Limnocalanus macrurus, Eurytemora affinis* and *Synchaeta* spp. in all treatments (**Figure 10**). On day 17, *L. macrurus* and *Bosmina coregoni maritima* made up on average ∼ 70 and ∼ 20% of the zooplankton biomass in the controls and ∼ 30 and ∼ 50% in the tM enriched treatments, respectively. At the end of the experiment, *B. coregoni maritima* dominated in the controls and tM_L treatment, while *B. coregoni maritima* and *L. macrurus* contributed equally ∼ 30% of the zooplankton biomass in tM_H.

During the second part of the experiment, the relative contribution of *L. macrurus* was positively correlated with bacterial biomass (Spearman's $\varrho = 0.60$, $p < 0.01$) and the relative contribution of picophytoplankton (Spearman's $\varrho = 0.49$, $p < 0.05$), as well as negatively correlated with ciliate biomass (Spearman's $\varrho = -0.54$, $p < 0.01$) and the relative contribution of nanophytoplankton (Spearman's $\varrho = -0.68$, $p < 0.01$). The relative contribution of *E. affinis* was positively correlated with the relative contribution of microphytoplankton (Spearman's $\varrho = 0.47$, $p < 0.05$), while the relative contribution of *B. coregoni maritima* increased with the higher relative contribution of nanophytoplankton (Spearman's $\varrho = 0.54$, $p < 0.01$) and decreased with higher bacterial biomass (Spearman's $\varrho = -0.46$, $p < 0.05$).

DISCUSSION

In natural aquatic ecosystems, the phytoplankton communities are controlled both by bottom-up and top-down factors (Andersson et al., 1996; Gruner et al., 2008; Hulot et al., 2014). In our study, the inorganic nutrient availability and light level played large roles in shaping the phytoplankton community. Among these two factors, the inorganic nutrient levels were found to be more important for the phytoplankton species composition and size-structure than the light levels. In the tM enriched mesocosms the nitrogen and phosphorus concentrations were 2-6-fold higher than in the controls, and in these mesocosms the phytoplankton community was dominated by microphytoplankton. On the contrary, picophytoplankton dominated the phytoplankton community in the controls. The results are in accordance with the theory that small cells have a competitive advantage at low inorganic nutrient concentrations (Raven, 1998), and that large phytoplankton cells have lower affinity for nutrients but higher maximum uptake capacity per cell under nutrient-rich conditions. Thus, in our experiment, inorganic nutrients were likely more important than light attenuation in shaping the size-structure of the phytoplankton community. Additionally, Bacillariophyceae and

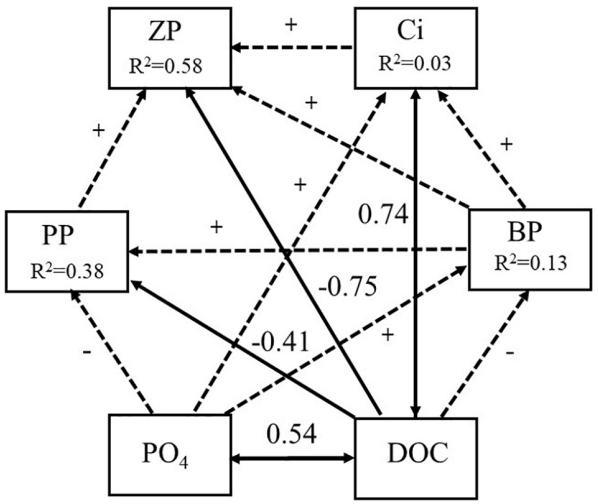

FIGURE 9 | Path diagram for structural equation model relating phosphate (PO_4) and dissolved organic carbon (DOC) to primary production (PP), bacterial production (BA), ciliate biomass (Ci) and zooplankton biomass (ZP) during the second part of the experiment (Day 17 and Day 28). Squared multiple correlation (R^2) in boxes indicate the percent of variance explained through the model. The numbers next to arrow are standardized regression coefficients of the SEM model. Solid black arrows represent significant path ($p < 0.05$) while dash arrows non-significant paths ($p > 0.05$). Plus or minus indicate relationship between variables.

picophytoplankton, prefer different inorganic nitrogen forms (Glibert and Berg, 2009; Glibert et al., 2016). Studies performed in river influenced estuaries or mesocosm experiments showed a positive correlation between the relative contribution of Bacillariophyceae and the proportion of NO_3 uptake while an increase in the picophytoplankton was related with NH_4 uptake (Glibert and Berg, 2009; Glibert et al., 2016).

The PAR levels were 2-12-fold higher in the controls than in the tM mesocosms (across the experiment), which in principle could have promoted small cells in the tM mesocosms. Picophytoplankton are more efficient in catching light at low light levels than large cells, due to their distribution of pigments along the outer cell membrane. The PAR levels were 4–33 μmol photon m^{-2} s^{-1} in the tM mesocosms, which would be below or near the photosynthetic saturation levels. A previous study performed in the same coastal area showed that pico- and nanophytoplankton photosynthesis saturates at ∼20 μmol photon m^{-2} s^{-1}, while microphytoplankton require 100–150 μmol photon m^{-2} s^{-1} for photosynthesis saturation (Andersson et al., 1994). These light level thresholds may vary due to physiological adaptations of the phytoplankton, but it still indicates that photosynthesis was saturated in the controls (PAR ∼50 μmol photon m^{-2} s^{-1}), on the edge of saturation in the tM_L treatment, and light limited in tM_H. However, we can conclude that light levels are of lower priority for governing the phytoplankton cell sizes than the nutrient levels, as microphytoplankton dominated in the inorganic nutrient-rich low-light tM-mesocosms and picophytoplankton dominated in the low-inorganic nutrient and high-light control-mesocosms.

We hypothesized that the photosynthetic efficiency, measured as the primary production to Chl *a* ratio, would decrease in the tM enriched mesocosms due to "overproduction" of chlorophyll

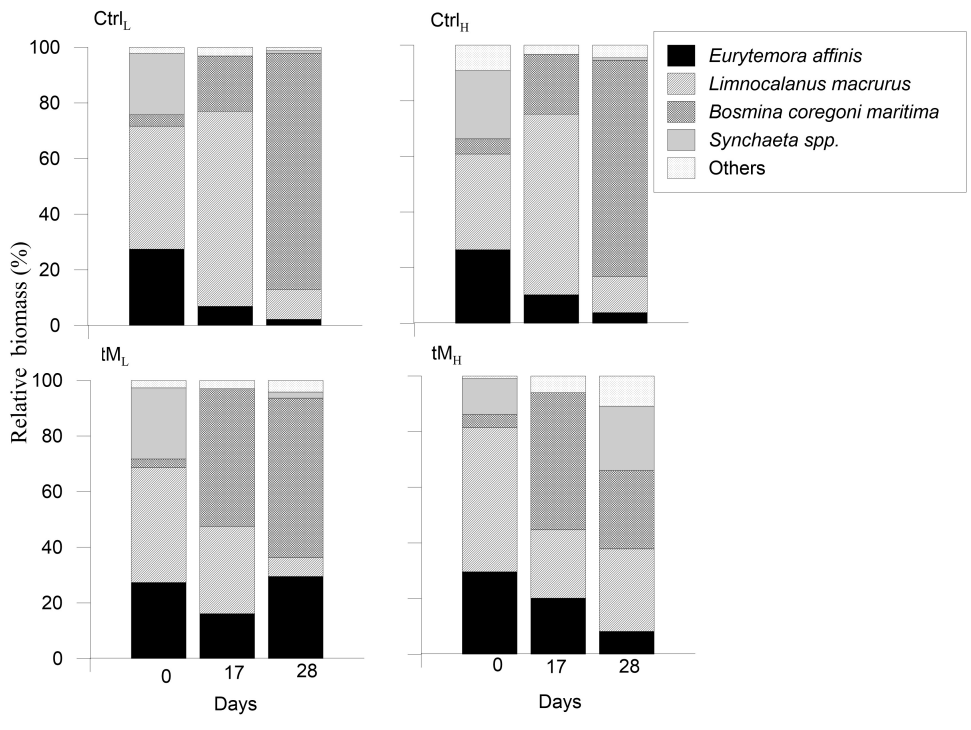

FIGURE 10 | Mesozooplankton taxonomic composition at the start, middle and end of the experiment (Day 0, Day 17, and Day 28) in all treatments.

to increase the light capture. This was indeed seen, even though there was a consecutive decrease of the photosynthetic efficiency from the low nutrient control to the high nutrient tM mesocosms (**Figure 7E**). Adjustment of the cell Chl *a* content is not only due to variations in the light level but also to other factors, such as alterations of the inorganic nutrient concentration (Geider et al., 1998; Staehr et al., 2002; Kirk, 2011). In fact, this is also what we observed in our experiment (**Figure 7E**). The Chl *a*:C ratios as well as the inorganic nutrient concentrations were lowest in the $Ctrl_L$ treatment and highest in tM_H. Additionally, the size-structure and taxonomic composition of the phytoplankton community have been shown to affect the cell Chl *a* content (Staehr et al., 2002). Smaller cells have higher Chl *a*:C ratios, due to larger surface-to-volume ratio and thus lower "self-shading" (Raven, 1998; Kirk, 2011). In our experiment a higher relative contribution of picophytoplankton was not followed by higher Chl *a*:C, suggesting that the higher chlorophyll content of the phytoplankton in the tM_H treatment was due to acclimation of larger cells rather than to changes in the phytoplankton size-structure.

The light levels were similar in the controls, while both the inorganic nutrient levels and Chl *a*:C ratio were slightly higher in the $Ctrl_H$ than in the $Ctrl_L$. This argues for a slightly higher role of inorganic nutrients than light, at least for the control mesocosms. High inorganic nutrient availability would allow the phytoplankton to allocate resources to build up their biomass and cell constituents including Chl *a*:C. Thus, in the tM-amended mesocosms light reduction in combination with high inorganic nutrient availability would drive the cells to produce higher amounts of chlorophyll.

Increased Chl *a* content of phytoplankton to maintain primary production at decreasing light levels was also a hypothesis of this experiment. This seems to be true in the low tM enriched mesocosms. In this treatment, the primary production was approximately as high as in the high nutrient control. However, the lowest primary production occurred in the high tM treatment. Under the higher level of tM addition the "overproduction" of Chl *a* did not help maintaining high primary production rates. If our experimental results also hold true in nature, then tM inflows causing DOC concentrations of ∼7–9 mg l^{-1} and humic substances concentrations exceeding 40 μg l^{-1}, may be disadvantageous for coastal primary production. Of course, the effect would depend on the depth of the water column, but in coastal areas with a water depth of a couple of meters, tM inflows of such magnitudes would have a negative effect on primary production. However, our results also indicate that tM inflows can have a positive effect on coastal primary production if the tM carries nutrients to the recipient system and DOC and humic substances loads are not exceeded. In general, our experimental results are in agreement with an earlier field study, where Andersson et al. (2018) found that in the upper part of an estuary in the northern Baltic Sea river-borne tM had a hindering effect on primary production when the DOC concentration exceeded 6 mg l^{-1}. Our results also match the proposed hump-shaped relationship between tM inflows to lake ecosystems and productivity (Seekell et al., 2015).

The SEM model provided a broad overview of the interactions taking place between major components of the food web and the major physicochemical drivers (phosphate and DOC). BP was identified as a positive pathway in relation to primary production, though likely the underlying interactions are more complex within these broad patterns reflecting the intricate balance between these biological components and common inorganic nutrient pools, and between the biological components themselves. In our study, both phytoplankton and heterotrophic bacterial growth depended on the same inorganic nutrient pool and phytoplankton were the major source of carbon for heterotrophs. Moreover, bacterial communities are also capable of releasing inorganic nutrients via the breakdown of organic matter, as was documented in this experiment (Traving et al., 2017), making the inorganic nutrient pool an even more critical factor, particularly in the tM treatments. DOC was identified as a major significant positive direct pathway for ciliate biomass, although a direct pathway via the microbial food web could not be confirmed. The SEM model showed also non-significant and negative pathway from DOC to BP, as well as significant and negative pathways from DOC to primary production and to zooplankton biomass. Thus, it is likely that the identified direct pathway from DOC to ciliate biomass overrode the measurable contribution of the microbial food web pathway since the tM additions were filtered through 90 μm mesh, likely providing a valuable source of particulate matter for ciliate biomass production. Though particulate matter was not measured in the experiment directly it was noted that the mesocosms receiving tM additions contained visible sedimentation by the end of the experiment and the particulate matter in question would have likely mirrored the DOC trends since the measured DOC values reflect the additions of tM (soil extract) that took place over the duration of the experiment.

In our experiment, picophytoplankton were positively correlated with mesozooplankton and negatively with ciliates, indicating that grazing exerted by higher trophic levels decreased predation pressure on the small cells (bacteria and picophytoplankton). Further, the proportion of nano- and microphytoplankton showed negative relationships with mesozooplankton, which were positively correlated with ciliates, as a consequence of the trophic cascade. This dynamic was observed mostly at the middle of the experiment, and did not differ markedly between the treatments, indicating that it was likely a general experimental effect, and not due to the addition of tM. In the Baltic Sea, field studies as well as mesocosm experiments have shown that the phytoplankton community is more driven by bottom-up than by top-down factors (Lagus et al., 2004; Legrand et al., 2015). Though mesozooplankton influenced the temporal phytoplankton dynamics, inorganic nutrients were the most important variables shaping phytoplankton composition and size-structure.

The mesozooplankton community seemed to be tightly linked to the taxonomic composition and size-structure of the phytoplankton community. Toward the end of the experiment, the cladoceran *Bosmina coregoni maritima* dominated the mesozooplankton community in the controls and the tM_L treatment. This zooplankton species is a filter-feeder known

to feed on small prey, pico- and nanophytoplankton (Bleiwas and Stokes, 1985; Korosi et al., 2013) and in our experiment *B. coregoni maritima* was observed to increase with the higher relative contribution of nanophytoplankton and decreased with higher bacterial biomass. The zooplankton community likely adapted to the phytoplankton size-structure, as in the controls and the tM_L treatment the pico- and nanophytoplankton constituted 50–95% of the total phytoplankton biomass. By the end of the experiment the zooplankton community in the tM_H treatment was equally distributed between *Synchaeta* spp., *B. coregoni maritima* and *Limnocalanus macrurus*. *L. macrurus* was the largest zooplankton taxa (>1000 μm) in the system, and it feeds on smaller zooplankton such as copepodites, nauplii and on larger phytoplankton (Warren, 1985). *L. macrurus* was positively correlated with bacterial biomass, the relative contribution of picophytoplankton and negatively with ciliate biomass and the relative contribution of nanophytoplankton. It is thus possible that *L. macrurus* fed on copepodites of *Eurytemora affinis*, which decreased toward the end of the experiment, as well as on *B. coregoni maritima* and other zooplankters. This could have been driven by high abundances of large diatoms that nurtured *Synchaeta* spp. and other zooplankton groups, which may have benefited from the dominance of large microphytoplankton. Taken together, it seems as if the composition of the mesozooplankton community was driven by phytoplankton size-structure, which in turn was governed by the inorganic nutrient availability. Furthermore, filter feeders may also have been supported by increased bacterial production and biomass in the tM treatments.

CONCLUSION

In conclusion, our study shows that phytoplankton size-structure and primary production were governed foremost by inorganic nutrients, including those associated with tM inputs, with light availability or grazing being secondary drivers. Higher tM promoted microphytoplankton, while the importance of picophytoplankton increased under nutrient limitation. Heterotrophic bacterial growth was tightly coupled with phytoplankton produced carbon. Furthermore, phytoplankton cells acclimated to lower light availability (e.g., moderate addition of tM) by increasing their cell chlorophyll content, allowing them to maintain photosynthetic efficiency at a similar level to the control conditions. This study demonstrates how variable the phytoplankton Chl *a*:C in coastal areas can be due to varying river inputs of freshwater, causing changes in the light and nutrient availability.

This study strongly indicates that an increase in river runoff, as predicted in future climate change scenarios for the region, would affect size-structure and production of phytoplankton depending on the amount of organic and inorganic nutrients associated with tM delivered to the ecosystem. Our study demonstrates that organic nutrients brought by the tM can be transformed to inorganic forms and utilized as growth substrate by coastal phytoplankton. The potential for climate related changes to have differing routes toward impacting higher trophic levels and ecosystem function are highlighted, and the potential for tipping points in the system due to reaching a critical load or light inhibition warrant further research.

DATA AVAILABILITY STATEMENT

The datasets generated for this study can be found in the Data Matrix.

ETHICS STATEMENT

Experiments, methods of sacrifices and design of fish sampling strategies in this study comply with the current laws of Sweden and were approved by the Regional Ethics Committee of the Swedish National Board for Laboratory Animals in Umeå (CFN, license no. A24-11).

AUTHOR CONTRIBUTIONS

All authors designed and performed the experiment. JP and AA took the lead writing the manuscript, and all authors contributed.

FUNDING

Access to the facility and project support was provided by the European Union Seventh Framework Program (FP7/2007-2013) under grant agreement 228224, MESOAQUA. Additionally, this study was supported by the Marine Strategic Research Environment EcoChange (the Swedish Research Council Formas) and the research program WATERS (the Swedish Agency for Marine and Water Management and the Swedish Environmental Protection Agency).

ACKNOWLEDGMENTS

We are grateful to the staff at the Umeå Marine Sciences Centre for their expert assistance, in particular Henrik Larsson for chemical analyses and mesocosm maintenance. We also appreciate the assistance given by Rickard Degerman, Ruaridh Hägglund, Fernanda Helena Bosco de Miranda Vasconcelos, Fidel Chiriboga, and Sachia J. Traving during the project, and thank Dr. Iveta Jurgensone for phytoplankton analysis and Dr. Liudmyla Guleikova for zooplankton analysis.

SUPPLEMENTARY MATERIAL

The Supplementary Material for this article can be found online at: https://www.frontiersin.org/articles/10.3389/fmars.2020.00080/full#supplementary-material

REFERENCES

Andersson, A., Brugel, S., Paczkowska, J., Figueroa, D., Rowe, O., Kratzer, S., et al. (2018). Influence of allochthonous dissolved organic matter on pelagic basal production in a northerly estuary. *Estuar. Coast. Shelf Sci.* 204, 225–235. doi: 10.1016/j.ecss.2018.02.032

Andersson, A., Haecky, P., and Hagström, A. (1994). Effect of temperature and light on the growth of micro- nano- and picoplankton: impact on algal succession. *Mar. Biol.* 120, 511–520. doi: 10.1007/bf00350071

Andersson, A., Hajdu, S., Haecky, P., Kuparinen, J., and Wikner, J. (1996). Succession and growth limitation of phytoplankton in the Gulf of Bothnia (Baltic Sea). *Mar. Biol.* 126, 791–801. doi: 10.1007/bf00351346

Andersson, A., Jurgensone, I., Rowe, O. F., Simonelli, P., Bignert, A., Lundberg, E., et al. (2013). Can humic water discharge counteract eutrophication in coastal waters? *PLoS One* 8:61293. doi: 10.1371/journal.pone.00061293

Andersson, A., Meier, H. E. M., Ripszam, M., Rowe, O., Wikner, J., Haglund, P., et al. (2015). Projected future climate change and Baltic Sea ecosystem management. *Ambio* 44(Suppl. 3), 345–356. doi: 10.1007/s13280-015-0654-8

Asmala, E., Autio, R., Kaartokallio, H., Pitkanen, L., Stedmon, C. A., and Thomas, D. N. (2013). Bioavailability of riverine dissolved organic matter in three Baltic Sea estuaries and the effect of catchment land use. *Biogeosciences* 10, 6969–6986. doi: 10.5194/bg-10-6969-2013

Asmala, E., Haraguchi, L., Jakobsen, H. H., Massicotte, P., and Carstensen, J. (2018). Nutrient availability as major driver of phytoplankton-derived dissolved organic matter transformation in coastal environment. *Biogeochemistry* 137, 93–104. doi: 10.1007/s10533-017-0403-0

Berggren, M., Ström, L., Laudon, H., Karlsson, J., Jonsson, A., Giesler, R., et al. (2010). Lake secondary production fueled by rapid transfer of low molecular weight organic carbon from terrestrial sources to aquatic consumers. *Ecol. Lett.* 13, 870–880. doi: 10.1111/j.1461-0248.2010.01483.x

Berglund, J., Müren, U., Båmstedt, U., and Andersson, A. (2007). Efficiency of a phytoplankton-based and a bacteria-based food web in a pelagic marine system. *Limnol. Oceanogr.* 52, 121–131. doi: 10.4319/lo.2007.52.1.0121

Bleiwas, A. H., and Stokes, P. M. (1985). Collection of large and small food particles by Bosmina. *Limnol. Oceanogr.* 30, 1090–1092. doi: 10.4319/lo.1985.30.5.1090

Carlsson, P., Graneli, E., Tester, P., and Boni, L. (1995). Influences of riverine humic substances on bacteria, protozoa, phytoplankton, and copepods in a coastal plankton community. *Mar. Ecol. Prog Ser.* 127, 213–221. doi: 10.3354/meps127213

Chust, G., Allen, J. I., Bopp, L., Schrum, C., Holt, J., Tsiaras, K., et al. (2014). Biomass changes and trophic amplification of plankton in a warmer ocean. *Glob. Chang. Biol.* 20, 2124–2139. doi: 10.1111/gcb.12562

Cowles, T. J., Olson, R. J., and Chisholm, S. W. (1988). Food selection by copepods: discrimination on the basis of food quality. *Mar. Biol.* 100, 41–49. doi: 10.1007/bf00392953

Dagg, M., Benner, R., Lohrenz, S., and Lawrence, D. (2004). Transformation of dissolved and particulate materials on continental shelves influenced by large rivers: plume processes. *Continent. Shelf Res.* 24, 833–858. doi: 10.1016/j.csr.2004.02.003

Dorado, S., Booe, T., Steichen, J., McInnes, A. S., Windham, R., Shepard, A., et al. (2015). Towards an understanding of the interactions between freshwater inflows and phytoplankton communities in a subtropical estuary in the Gulf of Mexico. *PLoS One* 10:e0130931. doi: 10.1371/journal.pone.0130931

Duarte, C. M., Agusti, S., and Agawin, N. S. R. (2000). Response of a mediterranean phytoplankton community to increased nutrient inputs: a mesocosm experiment. *Mar. Ecol. Prog. Ser.* 195, 61–70. doi: 10.3354/meps195061

Dubinsky, Z., and Stambler, N. (2009). Photoacclimation processes in phytoplankton: mechanisms, consequences, and applications. *Aquat. Microb. Ecol.* 56:2009.

Faithfull, C., Huss, M., Vrede, T., Karlsson, J., and Bergstrom, A. K. (2012). Transfer of bacterial production based on labile carbon to higher trophic levels in an oligotrophic pelagic system. *Can. J. Fish. Aquat. Sci.* 69, 85–93. doi: 10.1139/f2011-142

Falkowski, P. G., Katz, M. E., Knoll, A. H., Quigg, A., Raven, J. A., Schofield, O., et al. (2004). The evolutionary history of eukaryotic phytoplankton. *Science* 305, 354–360.

Field, C. B., Behrenfeld, M. J., Randerson, J. T., and Falkowski, P. (1998). Primary production of the biosphere: integrating terrestrial and oceanic components. *Science* 281, 237–240. doi: 10.1126/science.281.5374.237

Fuhrman, J. A., and Azam, F. (1982). Thymidine incorporation as a measure of heterotrophic bacterioplankton production in marine surface waters: evaluation and field results. *Mar. Biol.* 66, 109–120. doi: 10.1007/bf00397184

Gargas, E. (1975). *A Manual for Phytoplankton Primary Production Studies in the Baltic. The Baltic Marine Biologists, Publication No. 2*. Hørsholm: Water Quality Institute.

Geider, R. J., Macintyre, H. L., and Kana, T. M. (1998). A dynamic regulatory model of phytoplanktonic acclimation to light, nutrients, and temperature. *Limnol. Oceanogr.* 43, 679–694. doi: 10.4319/lo.1998.43.4.0679

Glibert, P. M., and Berg, G. M. (2009). "Nitrogen form, fate and phytoplankton composition," in *Experimental Ecosystems and Scale: Tools for Understanding and Managing Coastal Ecosystems*, eds V. S. Kennedy, W. M. Kemp, J. E. Peterson, and W. C. Dennison, (Cham: Springer), 183–189.

Glibert, P. M., Wilkerson, F. P., Dugdale, R. C., Raven, J. A., Dupont, C. L., Leavitt, P. R., et al. (2016). Pluses and minuses of ammonium and nitrate uptake and assimilation by phytoplankton and implications for productivity and community composition, with emphasis on nitrogen-enriched conditions. *Limnol. Oceanogr.* 61, 165–197. doi: 10.1002/lno.10203

Grasshoff, K., Ehrhardt, M., and Kremling, K. (1983). *Methods of Seawater Analysis, 2nd Revised and Extended Version*. Weinheim: Verlag Chemie.

Grubisic, L. M., Brutemark, A., Weyhenmeyer, G. A., Wikner, J., Båmstedt, U., and Bertilsson, S. (2012). Effects of stratification depth and dissolved organic matter on brackish bacterioplankton communities. *Mar. Ecol. Prog. Ser.* 453, 37–48. doi: 10.3354/meps09634

Gruner, D. S., Smith, J. E., Seabloom, E. W., Sandin, S. A., Ngai, J. T., Hillebrand, H., et al. (2008). A cross-system synthesis of consumer and nutrient resource control on producer biomass. *Ecol. Lett.* 11, 740–755. doi: 10.1111/j.1461-0248.2008.01192.x

Hägg, H. E., Humborg, C., Morth, C. M., Medina, M. R., and Wulff, F. (2010). Scenario analysis on protein consumption and climate change effects on riverine N export to the Baltic Sea. *Environ. Sci. Technol.* 44, 2379–2385. doi: 10.1021/es902632p

Hällfors, G. (2004). *Checklist of Baltic Sea phytoplankton Species*. Nairobi: United Nations Environment Programme.

Halsey, K. H., and Jones, B. M. (2015). Phytoplankton strategies for photosynthetic energy allocation. *Annu. Rev. Mar. Sci.* 7, 265–297. doi: 10.1146/annurev-marine-010814-015813

Hambright, K. D., Hairston, N. G. Jr., Schaffner, W. R., and Howarth, R. W. (2007). Grazer control of nitrogen fixation: synergisms in the feeding ecology of two freshwater crustaceans. *Fundam. Appl. Limnol.* 170, 89–101. doi: 10.1127/1863-9135/2007/0170-0089

Hernroth, L. (1985). Recommendations on methods for marine biological studies in the Baltic. Mesozooplankton biomass assessment. *Balt. Mar. Biol.* 10, 1–32.

Hoge, F. E., Vodacek, A., and Blough, N. V. (1993). Inherent optical properties of the ocean: retrieval of the absorption coefficient of chromophoric dissolved organic matter from airborne laser spectral fluorescence measurements. *Limnol. Oceanogr.* 38, 1394–1402. doi: 10.1364/AO.34.007032

Hulot, F. D., Lacroix, G., and Loreau, M. (2014). Differential responses of size-based functional groups to bottom-up and top-down perturbations in pelagic food webs: a meta-analysis. *Oikos* 123, 1291–1300. doi: 10.1111/oik.01116

Jónasdóttir, S. H. (2019). Fatty acid profiles and production in marine phytoplankton. *Mar. Drugs* 17:151. doi: 10.3390/md17030151

Kaartokallio, H., Asmala, E., Autio, R., and Thomas, D. N. (2016). Bacterial production, abundance and cell properties in boreal estuaries: relation to dissolved organic matter quantity and quality. *Aquat. Sci.* 78, 525–540. doi: 10.1007/s00027-015-0449-9

Kirk, J. T. O. (2011). *Light and Photosynthesis in Aquatic Ecosystems*. Cambridge: Cambridge University Press.

Kissman, C. E. H., Williamson, C. E., Rose, K. C., and Saros, J. E. (2013). Response of phytoplankton in an alpine lake to inputs of dissolved organic matter through nutrient enrichment and trophic forcing. *Limnol. Oceanogr.* 58, 867–880. doi: 10.4319/lo.2013.58.3.0867

Klug, J. L. (2002). Positive and negative effects of allochthonous dissolved organic matter and inorganic nutrients on phytoplankton growth. *Can. J. Fish. Aquat. Sci.* 59, 85–95. doi: 10.1139/f01-194

Korosi, J. B., Kurek, J., and Smol, J. P. (2013). A review on utilizing bosmina size structure archived in lake sediments to infer historic shifts in predation regimes. *J. Plankton Res.* 35, 444–460. doi: 10.1093/plankt/fbt007

Lagus, A., Suomela, J., Weithoff, G., Heikkila, K., Helminen, H., and Sipura, J. (2004). Species-specific differences in phytoplankton responses to N and P enrichments and the N: P ratio in the Archipelago Sea, northern Baltic Sea. *J. Plankton Res.* 26, 779–798. doi: 10.1093/plankt/fbh070

Lee, S., and Fuhrman, J. (1987). Relationship between biovolume and biomass of naturally derived bacterioplankton. *Appl. Environ. Microbiol.* 53, 1298–1303. doi: 10.1128/aem.53.6.1298-1303.1987

Lefébure, R., Degerman, R., Andersson, A., Larsson, S., Eriksson, L. O., Båmstedt, U., et al. (2013). Impacts of elevated terrestrial nutrient loads and temperature on pelagic food-web efficiency and fish production. *Glob. Chang. Biol.* 19, 1358–1372. doi: 10.1111/gcb.12134

Legendre, L., and Rassoulzadegan, F. (1995). Plankton and nutrient dynamics in marine waters. *Ophelia* 41, 153–172. doi: 10.1080/00785236.1995.10422042

Legrand, C., Fridolfsson, E., Bertos-Fortis, M., Lindehoff, E., Larsson, P., Pinhassi, J., et al. (2015). Microbial production in coastal and offshore food webs of the changing Baltic Sea. *Ambio* 44(Suppl. 3), 427–438.

Marañón, E. (2015). Cell size as a key determinant of phytoplankton metabolism and community structure. *Ann. Rev. Mar. Sci.* 7, 241–264. doi: 10.1146/annurev-marine-010814-015955

Marie, D., Simon, N., and Vaulot, D. (2005). "Phytoplankton cell counting by flow cytometry," in *Algal Culturing Techniques*, ed. R. A. Andersen, (San Diego: Academic Press), 253–267. doi: 10.1016/b978-012088426-1/50018-4

Markager, S. (1993). Light absorption and quantum yield for growth in 5 species of marine macroalgae. *J. Phycol.* 29, 54–63. doi: 10.1111/j.1529-8817.1993.tb00279.x

Masotti, I., Aparicio-Rizzo, P., Yevenes, M., Garreaud, R., Belmar, L., and Farías, L. (2018). The influence of river discharge on nutrient export and phytoplankton biomass off the Central Chile coast (33°-37°S). Seasonal cycle and interannual variability. In special issue marine microbiome and biogeochemical cycles in marine productive areas. *Front. Mar. Sci.* 5:423. doi: 10.3389/fmars.2018.00423

Meier, H. E. M., Muller-Karulis, B., Andersson, H. C., Dieterich, C., Eilola, K., Gustafsson, B. G., et al. (2012). Impact of climate change on ecological quality indicators and biogeochemical fluxes in the Baltic Sea: a multi-model ensemble study. *Ambio* 41, 558–573. doi: 10.1007/s13280-012-0320-3

Menden-Deuer, S., and Lessard, E. J. (2000). Carbon to volume relationships for dinoflagellates, diatoms, and other protist plankton. *Limnol. Oceanogr.* 45, 569–579. doi: 10.4319/lo.2000.45.3.0569

Meunier, C. L., Boersma, M., Wiltshire, K. H., and Malzahn, A. M. (2016). Zooplankton eat what they need: copepod selective feeding and potential consequences for marine systems. *Oikos* 125, 50–58. doi: 10.1111/oik.02072

Nordbäck, J., Lundberg, E., and Christie, W. W. (1998). Separation of lipid classes from marine particulate material by HPLC on a polyvinyl alcohol-bonded stationary phase using dual-channel evaporative light-scattering detection. *Mar. Chem.* 60, 165–175. doi: 10.1016/s0304-4203(97)00109-6

Olenina, I., Hajdu, S., Edler, L., Andersson, A., Wasmund, N., Busch, S., et al. (2006). Biovolumes and size-classes of phytoplankton in the Baltic Sea. *HELCOM Balt. Sea Environ. Proc.* 106:144.

Peltomaa, E. L., Aalto, S. L., Vuorio, K. M., and Taipale, S. J. (2017). The importance of phytoplankton biomolecule availability for secondary production. *Front. Ecol. Evol* 5:128. doi: 10.3389/fevo.2017.00128

Penna, N., Capellacci, S., and Ricci, F. (2004). The influence of the Po River discharge on phytoplankton bloom dynamics along the coastline of Pesaro (Italy) in the Adriatic Sea. *Mar. Pollut. Bull.* 48, 321–326. doi: 10.1016/j.marpolbul.2003.08.007

Rasconi, S., Gall, A., Winter, K., and Kainz, M. J. (2015). Increasing water temperature triggers dominance of small freshwater plankton. *PLoS One* 10:e0140449. doi: 10.1371/journal.pone.0140449

Raven, J. A. (1998). The twelfth tansley lecture. small is beautiful: the picophytoplankton. *Funct. Ecol.* 12, 503–513. doi: 10.1046/j.1365-2435.1998.00233.x

Riemann, B. (1985). Potential importance of fish predation and zooplankton grazing on natural populations of freshwater bacteria. *Appl. Environ. Microbiol.* 50, 187–193. doi: 10.1128/aem.50.2.187-193.1985

Roelke, D. L., Li, H. P., Hayden, N. J., Miller, C. J., Davis, S. E., Quigg, A., et al. (2013). Co-occurring and opposing freshwater inflow effects on phytoplankton biomass, productivity and community composition of Galveston Bay, USA. *Mar. Ecol. Prog. Ser.* 477, 61–76. doi: 10.3354/meps10182

Sanders, R. W., Caron, D. A., and Berninger, U. G. (1992). Relationships between bacteria and heterotrophic nanoplankton in marine and fresh waters: an inter-ecosystem comparison. *Mar. Ecol. Prog. Ser.* 86, 1–14. doi: 10.3354/meps086001

Schatz, G. S., and McCauley, E. (2007). Foraging behavior by Daphnia in stoichiometric gradients of food quality. *Oecologia* 153, 1021–1030. doi: 10.1007/s00442-007-0793-0

Schweitzer, B., and Simon, M. (1995). Growth limitation of planktonic bacteria in a large mesotrophic lake. *Microb. Ecol.* 30, 89–104. doi: 10.1007/BF00184516

Seekell, D. A., Lapierre, J. F., Ask, J., Bergstrom, A. K., Deininger, A., Rodriguez, P., et al. (2015). The influence of dissolved organic carbon on primary production in northern lakes. *Limnol. Oceanogr.* 60, 1276–1285. doi: 10.1002/lno.10096

Shangguan, Y., Glibert, P. M., Alexander, J. A., Madden, C. J., and Mursako, S. (2017a). Nutrients and phytoplankton in semienclosed lagoon systems in Florida Bay and their responses to changes in flow from Everglades restoration. *Limnol. Oceanogr.* 62, 327–347.

Shangguan, Y., Glibert, P. M., Alexander, J. A., Madden, C. J., and Murasko, S. (2017b). Phytoplankton assemblage response to changing nutrients in Florida Bay: results of mesocosm studies. *J. Exp. Mar. Biol. Ecol.* 494, 38–53. doi: 10.1016/j.jembe.2017.05.006

Sommer, U., Stibor, H., Katechakis, A., Sommer, F., and Hansen, T. (2002). Pelagic food web configurations at different levels of nutrient richness and their implications for the ratio fish production: primary production. *Hydrobiologia* 484, 11–20. doi: 10.1007/978-94-017-3190-4_2

Staehr, P. A., Henriksen, P., and Markager, S. (2002). Photoacclimation of four marine phytoplankton species to irradiance and nutrient availability. *Mar. Ecol. Prog. Ser.* 238, 47–59. doi: 10.3354/meps238047

Straile, D. (1997). Gross growth efficiencies of protozoan and metazoan zooplankton and their dependence on food concentration, predator-prey weight ratio, and taxonomic group. *Limnol. Oceanogr.* 42, 1375–1385. doi: 10.4319/lo.1997.42.6.1375

Swarbrick, V. J., Simpson, G. L., Glibert, P. M., and Leavitt, P. R. (2019). Differential stimulation and suppression of phytoplankton growth by ammonium enrichment in eutrophic hardwater lakes over 16 years. *Limnol. Oceanogr.* 64, 130–149.

Tikkanen, T., and Willen, T. (1992). *Phytoplankton Flora*. Solna: The Swedish Environmental Protection Agency.

Traving, S. J., Jakobsen, N. M., Sorensen, H., Dinasquet, J., Stedmon, C. A., Andersson, A., et al. (2017). The effect of increased of increase loads of dissolved organic matter on estuarine microbial community composition and function. *Front. Microbiol.* 8:351. doi: 10.3389/fmicb.2017.00351

Utermöhl, H. (1958). Zur vervollkommnung der quantitativen phytoplankton-methodik. *Verh. Int. Ver. Theor. Angew. Limnol.* 9, 1–38. doi: 10.1080/05384680.1958.11904091

Vrede, K. (1999). Effects of inorganic nutrients and zooplankton on the growth of heterotrophic bacterioplankton – enclosure experiments in an oligotrophic clearwater lake. *Aquat. Microb. Ecol.* 18, 133–144. doi: 10.3354/ame018133

Walve, J., and Larsson, U. (1999). Carbon, nitrogen and phosphorus stoichiometry of crustacean zooplankton in the Baltic Sea: implications for nutrient recycling. *J. Plankton Res.* 21, 2309–2321. doi: 10.1093/plankt/21.12.2309

Warren, G. J. (1985). Predaceous feeding habits of *Limnocalanus macrurus*. *J. Plankton Res.* 7, 537–552. doi: 10.1093/plankt/7.4.537

Wasmund, N. (2002). "Harmful algal blooms in coastal waters of the south-eastern Baltic Sea," in *Baltic Coastal Ecosystems*, eds G. Schernewski, and U. Schiewer, (Berlin: Springer), 93–116. doi: 10.1007/978-3-662-04769-9_8

Wikner, J., and Hagström, A. (1999). Bacterioplankton intra-annual variability: importance of hydrography and competition. *Aquat. Microb. Ecol.* 20, 245–260. doi: 10.3354/ame020245

Conflict of Interest: The authors declare that the research was conducted in the absence of any commercial or financial relationships that could be construed as a potential conflict of interest.